RandomRooms: Unsupervised Pre-training from Synthetic Shapes and Randomized Layouts for 3D Object Detection

Yongming Rao[1]*, Benlin Liu[2,3]*, Yi Wei[1], Jiwen Lu[1†], Cho-Jui Hsieh[2], Jie Zhou[1]

[1]Tsinghua University, [2]UCLA, [3]University of Washington

raoyongming95@gmail.com; liubl@cs.washington.edu; wziyi20@mails.tsinghua.edu.cn;

chohsieh@cs.ucla.edu; {lujiwen, jzhou}@tsinghua.edu.cn

Abstract

3D point cloud understanding has made great progress in recent years. However, one major bottleneck is the scarcity of annotated real datasets, especially compared to 2D object detection tasks, since a large amount of labor is involved in annotating the real scans of a scene. A promising solution to this problem is to make better use of the synthetic dataset, which consists of CAD object models, to boost the learning on real datasets. This can be achieved by the pre-training and fine-tuning procedure. However, recent work on 3D pre-training exhibits failure when transfer features learned on synthetic objects to other real-world applications. In this work, we put forward a new method called RandomRooms to accomplish this objective. In particular, we propose to generate random layouts of a scene by making use of the objects in the synthetic CAD dataset and learn the 3D scene representation by applying object-level contrastive learning on two random scenes generated from the same set of synthetic objects. The model pre-trained in this way can serve as a better initialization when later fine-tuning on the 3D object detection task. Empirically, we show consistent improvement in downstream 3D detection tasks on several base models, especially when less training data are used, which strongly demonstrates the effectiveness and generalization of our method. Benefiting from the rich semantic knowledge and diverse objects from synthetic data, our method establishes the new state-of-the-art on widely-used 3D detection benchmarks ScanNetV2 and SUN RGB-D. We expect our attempt to provide a new perspective for bridging object and scene-level 3D understanding.

1. Introduction

Recent years have witnessed great progress in 3D deep learning, especially on 3D point clouds. With the emer-
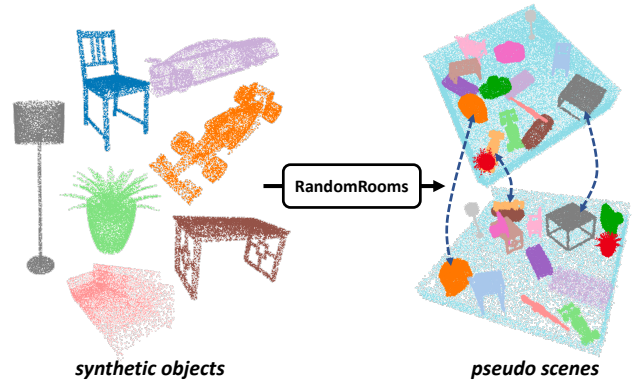

Figure 1: The main idea of *RandomRooms*. To generate two different layouts, we randomly place the same set of objects sampled from synthetic datasets in rectangular rooms. With the proposed object-level contrastive learning, models pre-trained on these pseudo scenes can serve as a better initialization for downstream 3D object detection task.

gence of powerful models, we are now able to make significant breakthroughs on many point cloud tasks, ranging from object-level understanding ones [24, 53, 27, 29] to scene-level understanding ones, such as 3D object detection [45, 59, 28, 44] and 3D semantic segmentation [25, 62, 21, 4, 19]. These scene-level tasks are considered to be more complicated and more important as they often require higher level understanding compared to object level tasks like shape classification. One of the most important tasks for 3D point cloud scene understanding is the 3D object detection, which aims at localizing the objects of interest in the point cloud of the scene and telling the category they belong to. However, one major bottleneck that hinders the researchers from moving forward is the lack of large-scale real datasets, considering the difficulty in collecting and labeling high-quality 3D scene data. Compared to 2D object detection task where we have large annotated real datasets COCO [30], the real datasets here we use for 3D object detection task are much smaller in scales, and generating a

arXiv:2108.07794v1 [cs.CV] 17 Aug 2021

synthesized scene dataset also involves a heavy workload in modeling and rendering.

A preferred solution is to utilize synthetic CAD object models to help the learning of 3D object detector since it is much easier to access such type of data. Considering we have no annotation of bounding box for synthetic CAD data, this idea can be achieved in a similar way as the unsupervised pre-training for 2D vision tasks where we first pretrain on a large-scale dataset in an unsupervised manner and then fine-tune on a smaller annotated dataset. Yet, most previous works focus on the pre-training for single object level tasks [31, 58, 6, 11, 40], such as reconstruction, shape classification or part segmentation, or on some low-level tasks like registration [6, 61, 10]. A recent work [57], namely PointContrast, first explores the possibility of pre-training in the context of 3D representation learning for higher level scene understanding tasks, i.e. 3D detection and segmentation. Nevertheless, they conduct the pre-training on the real scene dataset and provide a failure case when pre-training the backbone model on ShapeNet [1], which consists of synthetic CAD object models. They attribute this unsuccessful attempt to two reasons, that is, the domain gap between real and synthetic data as well as the insufficiency of capturing point-level representation by directly training on single objects. Despite these difficulties, it is still desirable to make the ShapeNet play the role of ImageNet in 2D vision since it is easy to obtain a large number of synthetic CAD models.

In this work, we put forward a new framework to show the possibility of using a synthetic CAD model dataset, i.e. ShapeNet, for the 3D pre-training before fine-tuning on downstream 3D object detection task. To this end, we propose a method named RandomRoom. In particular, we propose to generate two different layouts using one set of objects which are randomly sampled out of the ShapeNet dataset. Having these two scenes that are made up of the same set of objects, we can then perform the contrastive learning at the object level to learn the 3D scene representation.

Different from PointContrast [57] where the contrastive learning is performed at the point level, our approach has two advantages. One is to remove the requirement of point correspondence between two views, which is indispensable in PointContrast framework given that it is necessary to exploit such information to obtain positive and negative pairs for the contrastive learning. This requirement limits the applications of PointContrast, since the CAD model datasets like ShapeNet and many other real-world datasets like SUN RGB-D [47] cannot provide such information. The other advantage is that our method can support more diverse backbone models. Most state-of-the-art models [34, 35, 44] on tasks like 3D object detection apply PointNet++ [38] style models as their backbone, and replacing it with Sparse

Res-UNet may lead to the drop of accuracy, according to the PointContrast. However, PointContrast cannot well support the pre-training of PointNet++ style model as the UNet-like models, since the point correspondence may be missing after each abstraction level in PointNet++. With the proposed RandomRoom, we are enabled to perform contrastive learning at the level of objects and thus better support the pre-training of PointNet++ like models as we no longer need to keep the point correspondence for contrastive learning like PointContrast.

Our method is straightforward yet effective. We conduct the experiments on the 3D object detection task where only the geometric information is available for input as the models in CAD datasets do not carry color information. The results of empirical study strongly demonstrate the effectiveness of our method. In particular, we achieve the state-of-the-art of 3D object detection on two widely-used benchmarks, ScanNetV2 and SUN-RGBD. Furthermore, our method can achieve even more improvements when much less training samples are used, demonstrating that our model can learn a better initialization for 3D object detection.

2. Related Work

3D Deep Learning. 3D deep learning [22, 40, 45, 59, 28, 44, 19, 52, 54] has attracted much attention in recent years, especially on 3D point cloud analysis [37, 38, 24, 53, 27, 29]. As the pioneer work, PointNet [37] introduces deep learning to 3D point cloud analysis . With the max pooling layer, it is able to directly operate on unordered set. As a follow up, PointNet++ [38] employs PointNet as a basic module to hierachically extract features. Different from [37, 38]. Many other variants of PointNet++ are also devised to further improve feature capacity [24, 49]. Thanks to these architectures, significant processes have been made in many 3D applications [24, 53, 27, 29, 44, 35, 19, 52]. As the data-driven methods, these works either use object-level synthetic training data or leverage point clouds from real scenes. Exploring the great power of both synthetic and real-world datasets, our method bridges the gaps between object and scene level 3D understanding.

3D Object Detection. Due to the broad real-world applications, more and more works [45, 59, 28, 44, 19, 52, 57] focus on 3D scene understanding. As a fundamental 3D task, 3D object detection focuses on the problem of detecting objects' tight bounding boxes in 3D space. F-PointNet [36] predicts 3D bounding boxes from the points in frustums and achieves efficiency as well as high recall for small objects. It can also handle strong occlusion or cases with very sparse points. Inspired by Hough voting process, VoteNet [35] leverages voting mechanism to capture scene context around objects centers. Based on VoteNet, H3DNet [63]
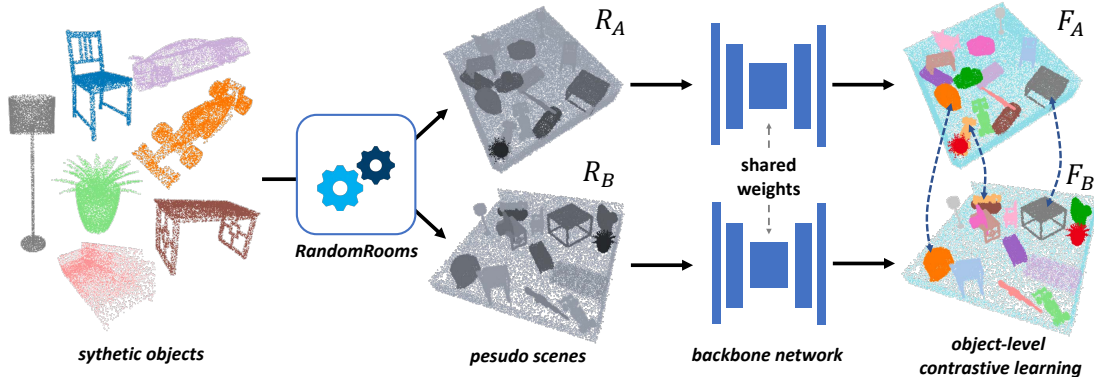
Figure 2: The overview of our framework. Given the objects randomly sampled from synthetic datasets, pairs of pesudo scenes are constructed following object augmentation, layout generation and scene augmentation. We pretrain the model with shared weights on two corresponding random rooms. An object-level contrastive learning (OCL) method is proposed to help the network learn discriminative representation.

predicts different modalities of geometric primitives and aggregate them to generate final 3D bounding boxes. Benefiting from hybrid features, H3DNet achieves state-of-the-art performance. However, these 3D scene understanding methods mainly make use of the real data from 3D sensors. On the contrary, our method aims at bringing the semantic knowledge in synthetic datasets to high-level 3D understanding tasks.

Model Pre-training. Pre-training has been the common practice for many machine learning tasks, ranging from vision [57, 2, 17, 3, 51, 13] to NLP tasks [33, 39, 20, 8]. In the context of 2D vision, the pre-training is often conducted on ImageNet [7] with full supervision, and we can then fine-tune the pre-trained backbone model on downstream tasks like detection [13, 41, 12]. More recently, unsupervised pre-training on ImageNet [2, 17, 3] has been been showed to be effective. Compared to 2D vision, less exploration has been made on 3D vision tasks. Previously, most methods on 3D pre-training either focus on the tasks at single object level, like classification, reconstruction and part segmentation [58, 11, 40, 16], or on some low-level 3D tasks like registration [6, 61, 10]. Pre-training for higher level 3D scene understanding tasks like detection and segmentation has not been studied only until a recent work [57], which exploits the point correspondence to learn the representation in an unsupervised manner. Compared to theirs, our method can pre-train on synthetic CAD datasets like ShapeNet and support more types of backbone model.

3. RandomRooms

In this section, we describe the details of the proposed RandomRooms method. We first briefly review existing contrastive representation learning methods and illustrate the intuition of our method in Section 3.1. Then, we describe how to use synthetic objects to construct random

rooms in 3.2. In Section 3.3, we show our pretrain task for learning scene level representation from the pseudo scenes. The overview of our framework is presented in Figure 2.

3.1. Overview of Contrastive Learning

We begin by reviewing the existing contrastive representation learning methods for 2D and 3D understanding to illustrate the motivation of our method.

Contrastive learning is at the core of several recent methods on unsupervised learning, which exhibits promising performance on both 2D [56, 18, 50, 17, 3, 2, 14, 51] and 3D [57, 40] tasks and shows impressive generalization ability as a new type of pre-training method for various downstream tasks. The key ingredient of contrastive learning is constructing positive and negative pairs to learn discriminative representation, which inherits the idea of conventional contrastive learning in metric learning literature [15]. Given an input x and its positive pair x_+ and a set of negative examples $\{x_i\}$, a commonly used training objective for contrastive representation learning is based on InfoNCE [18, 50]:

$$\mathcal{L}_{\text{contrastive}} = -\log \frac{\exp(\varphi(x) \cdot \varphi(x_+)/\tau)}{\sum_i \exp(\varphi(x) \cdot \varphi(x_i)/\tau)}, \quad (1)$$

where φ is the encoder network that maps the input to a feature vector and τ is a temperature hyper-parameter following [56, 17, 2]. Intuitively, the contrastive learning methods supervise models by encouraging the features of the different *views* of the same sample to be close to each other and distinguishable from other samples [46, 43]. Hence the quality of positive pairs and negative examples is a critical factor to learn the encoder.

Since category annotations are not available in the unsupervised learning scenario, a common practice [9, 56, 17] is using different augmentations of an input as the positive
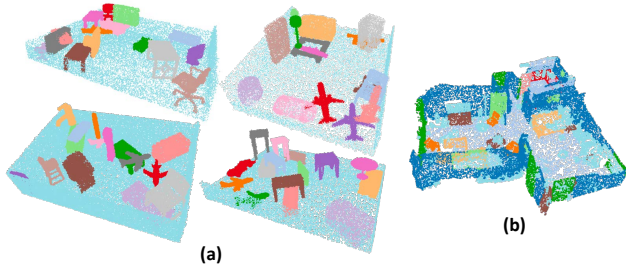
Figure 3: Some randomly selected examples of random rooms (a) and scene from ScanNetV2 (b).

pairs and treating all other samples as negative examples. Although this design has proven to be effective in image representation learning, we argue there is a better solution to construct positive pairs for 3D understanding. One fundamental difference between 2D and 3D data is that the spatial structures of pixels do not reflect the actual geometric structures of the objects, but the spatial structures in 3D data always faithfully illustrate the layouts in the real world. This property suggests that it may be easier to manipulate or *augment* 3D data compared to 2D images. Inspired by the rendering techniques in computer graphics, we propose to generate positive pairs of 3D scenes by randomly manipulating the layouts of 3D objects in a scene. Since we only need 3D objects instead of the whole scene in this process, our method makes it possible to use 3D object models to promote scene level representation learning.

It is worth noting that a recent work, namely PointContrast [57], explores 3D contrastive representation learning by using 3D point clouds from different views as the positive pair, where a point level contrastive loss is designed. This method is based on the multi-view point cloud sequences provided in ScanNetV2 [5]. Instead, our method focuses on leveraging object level 3D data, which are easier to collect and have more diverse categories.

3.2. Random Rooms from Synthetic Objects

Compared to ScanNetV2 [5], which contains ∼15k objects from 17 categories, synthetic shape datasets like ShapeNet [55] provide a more plentiful source for 3D understanding. For example, ShapeNetCore [55] contains ∼52k objects from 55 categories). Therefore, the primary goal of this paper is to study how to use synthetic CAD models collected by ShapeNet to improve downstream tasks like 3D detection and segmentation on real-world datasets.

Previous work [57] shows that directly pre-training on ShapeNet will not yield performance improvement on downstream detection and segmentation task. We suspect the main reason is the domain gap between the single object classification task on ShapeNet and the multiple objects localization task on real-world datasets. In order to bridge the gap, we propose to generate pseudo scenes (we name them

as ***random rooms***) from synthetic objects to construct the training data that are helpful for scene level understanding.

Given a set of randomly sampled objects, we generate a random room following the three steps:

- **Object Augmentation:** We first resize the object to a random size in [0.5m, 2.0m] to ensure the objects have similar sizes as the objects in ScanNetV2. Then, we apply commonly used object point cloud augmentation techniques [37, 38, 32] including rotation, point dropping, jittering.

- **Layout Generation:** For the ease of implementation, we place objects in a rectangular room. The size of the room is adaptively adjusted according to the overall area of the augmented objects. The layout is generated based on two simple principles: 1) non-overlapping: any two objects should not occupy the same space in the room; 2) gravity: objects should not float in the air, and larger objects should not be placed over the smaller ones. In turn, we place objects in the descending order of the area. Inspired by *Tetris* [1], for each object, we first randomly choose a position in the X-Y plane that satisfies the above principles, then determine the location (the Z value) based on the current maximum height of the position. The object will not be placed in a position if the current maximum height of the position exceeds 2m.

- **Scene Augmentation:** Lastly, we apply data augmentation like rotation along the Z axis, point dropping, jittering to the whole scene. To make the generated scenes more similar to the real scenes, we also add the floor and walls as confounders.

Some examples of the random rooms are illustrated in Figure 6.

3.3. Representation Learning from Random Rooms

To utilize the generated random rooms, we devise an object-level contrastive learning (OCL) method, which learns discriminative representation without category annotations.

Given n randomly sampled objects $\{x_1, x_2, ..., x_n\}$, we first generate two random rooms $R_A = \{x_1^A, x_2^A, ..., x_n^A\}$ and $R_B = \{x_1^B, x_2^B, ..., x_n^B\}$ by conducting the above-mentioned steps individually. Then, we employ the point cloud encoder-decoder network $\mathcal{M}$ (*e.g.* PointNet++ [38] with feature propagation layers) to extract per-point features of the two scenes $F_A = \mathcal{M}(R_A)$ and $F_B = \mathcal{M}(R_B)$. Since the random room is constructed by several individual objects, the instance labels can be naturally defined. The goal of object-level contrastive learning is to exploit the instance

---

[1]https://en.wikipedia.org/wiki/Tetris

labels as a source of free and plentiful supervisory signals for training a rich representation for point cloud understanding. To obtain the feature of each object, we apply the average pooling operation $\mathcal{A}$ on per-point features belonging to this object:

$$\{h_1^A, h_2^A, ..., h_n^A\} = \mathcal{A}(F_A), \quad \{h_1^B, h_2^B, ..., h_n^B\} = \mathcal{A}(F_B).$$

Similar to the common practice in contrastive learning [3, 2], the object features then are projected onto a unit hypersphere using a multi-layer perceptron network (MLP) followed by L2 normalization. The object-level contrastive learning objective can be written as:

$$\begin{aligned}
\mathcal{L}_{\text{OCL}} = &- \frac{1}{n} \sum_{i=1}^{n} \log \frac{\exp(f_i^A \cdot f_i^B / \tau)}{\sum_{f \in \mathcal{F}} \exp(f_i^A \cdot f / \tau)} \\
&- \frac{1}{n} \sum_{i=1}^{n} \log \frac{\exp(f_i^B \cdot f_i^A / \tau)}{\sum_{f \in \mathcal{F}} \exp(f_i^B \cdot f / \tau)},
\end{aligned} \quad (2)$$

where $f_i^A = \phi(h_i^A)$ and $f_i^B = \phi(h_i^B)$ are the projected features of the i-th object in R_A and R_B respectively, ϕ is the projection head, and $\mathcal{F}$ is the set of all projected features in the batch. Note that compared to point-level contrastive learning task in PointContrast [57], our method further utilizes the instance-level knowledge thanks to the generation mechanism of RandomRooms. We argue that object-level contrastive learning introduces more semantic knowledge and can be more helpful for downstream localization tasks (Some empirical evidence can be found in Table 5b).

4. Experiments

One primary goal of representation learning is to learn representation that can transfer to downstream tasks. To apply our RandomRooms method to scene level understanding task like 3D object detection, we adopt the *unsupervised pre-training + supervised fine-tuning* pipeline [17, 57]. Specifically, we first pre-train the backbone model on ShapeNet using our method, then we use the pre-trained weights as the initialization and further fine-tune the model on the downstream 3D object detection task.

4.1. Pre-training Setups

We perform the pre-training on ShapeNet [1], a dataset composed of richly-annotated shapes represented by 3D CAD models of objects from 55 common categories. To generate the random room, we first need to randomly sample multiple objects from the the dataset. The number of objects we sample is a random integer from 12 to 18, which is similar to the average number of objects in ScanNetV2 scenes. Then for each sampled object, we perform the random room generation algorithm mentioned in Section 3.2. The object-level contrastive learning loss is used to train the model in an unsupervised manner.

For the downstream 3D object detection task, we use the backbone models proposed in [35] and [63], which take as input 40,000 points. Following the network configurations in these two works, we use the 1024-point feature as the output of the backbone models and perform contrastive learning on this feature. During pre-training, we use the Adam optimizer [23] with initial learning 0.001. We train the model for 300 epochs and the learning rate is multiplied by 0.1 at the 100-th and 200-th epcoh. The batch size is set to 16 such that roughly 200~300 unique objects are involved in the contrastive learning at every iteration.

4.2. 3D Object Detection

Datasets. We conduct experiments on two widely-used 3D detection benchmarks, ScanNetV2 [5] and SUN-RGBD [47]. ScanNetV2 is a richly annotated dataset of 3D reconstructed meshes of indoor scenes. It contains 1,513 scanned and reconstructed real scenes, which consists of 18 different categories of objects of various size and shape. Currently, it is the largest one that was created with a lightweight RGB-D scanning procedure. Yet, it is still much smaller in scale when compared to datasets in 2D vision. We split the the whole dataset into two subsets with 1,201 and 312 scenes for training and testing following [35, 5]. SUN RGB-D is a single-view RGB-D dataset for 3D scene understanding. It contains of 10,335 indoor RGB and depth images with object bounding boxes and per-point semantic labels with 10 different categories of objects. We also strictly follow the splits described in [35, 5], with 5,285 samples as training data and 5,050 as testing data.

Detection Models. We compare our method with two recently proposed state-of-the-art approaches: One is VoteNet [35], which is a geometric-only detector that combines deep point set networks and a voting procedure; the other is H3DNet, which predicts a hybrid set of geometric primitives. Both of them take colorless 3D point clouds as input. We also include GSPN [60], 3D-SIS [19], DSS [48], F-PointNet [36], 2D-Driven [26], and Cloud of gradient (COG) [42], which use other types of information for object detection, into the comparison.

Implementation Details. We show the effectiveness of our method by the improvement upon VoteNet and H3DNet. We load the pre-trained part into the model at the beginning of the training, and follow their training setting. Specifically, we train the model for 360 iterations in total. The initial learning is 1e-2 and 1e-3 for ScanNetV2 and SUN-RGBD respectively. We evaluate the performance by mAP with 3D IoU threshold as 0.25 and 0.5. Please refer the original paper for more details with regard to the experimental settings.

ScanNetV2. We first report the results of mAP@0.25 as well as AP@0.25 for all semantic classes in Table 1. With

Table 1: 3D object detection results on ScanNetV2 validation set. Per-category results of average precision (AP) with IOU threshold 0.25 are reported. We also show the mean of AP across all semantic classes with IoU threshold 0.25.

	Input	cab	bed	chair	sofa	tabl	door	wind	bkshf	pic	cntr	desk	curt	fridg	showr	toil	sink	bath	ofurn	mAP
3DSIS-5[19]	Geo+RGB	19.8	69.7	66.2	71.8	36.1	30.6	10.9	27.3	0.0	10.0	46.9	14.1	53.8	36.0	87.6	43.0	84.3	16.2	40.2
3DSIS[19]	Geo	12.8	63.1	66.0	46.3	26.9	8.0	2.8	2.3	0.0	6.9	33.3	2.5	10.4	12.2	74.5	22.9	58.7	7.1	25.4
Votenet[35]	Geo	36.3	87.9	88.7	89.6	58.8	47.3	38.1	44.6	7.8	56.1	71.7	47.2	45.4	57.1	94.9	54.7	92.1	37.2	58.6
Ours + VoteNet	Geo	37.2	87.4	88.9	89.8	61.9	45.3	42.6	53.5	7.8	51.7	67.2	53.5	54.0	66.4	96.8	62.6	92.0	43.6	61.3
H3DNet[63]	Geo	49.4	88.6	91.8	90.2	64.9	61.0	51.9	54.9	18.6	62.0	75.9	57.3	57.2	75.3	97.9	67.4	92.5	53.6	67.2
Ours + H3DNet	Geo	53.6	89.7	92.1	90.1	71.5	58.2	54.2	53.0	16.6	60.5	79.1	56.1	58.1	85.0	98.8	71.1	89.5	57.4	**68.6**

Table 2: 3D object detection results on ScanNetV2 validation set. We show mean of average precision (mAP) across all semantic classes with 3D IoU threshold 0.25 and 0.5.

	Input	mAP$_{25}$	mAP$_{50}$
DSS[48]	Geo + RGB	15.2	6.8
F-PointNet[36]	Geo + RGB	19.8	10.8
GSPN[60]	Geo + RGB	30.6	17.7
3D-SIS [19]	Geo + 5 views	40.2	22.5
PointContrast [57]	Geo only	58.5	38.0
VoteNet [35]	Geo only	58.6	33.5
Ours + VoteNet	Geo only	61.3	36.2
H3DNet [63]	Geo only	67.2	48.1
Ours + H3DNet	Geo only	68.6	51.5

the pre-training, we improve the mAP by 2.6 point and 1.4 points for VoteNet and H3DNet respectively. These results indicate that our pre-training can truly improve the fine-tuning on high-level detection tasks. Moreover, for 11 out of 18 categories, improvement of the average precision can be observed. This indicates the pre-training can boost the detection of most common categories.

We further report the results of mAP@0.5, which is a more difficult metric, and add the comparison with other 3D object detection approaches that utilize the color information in Table 2. For both mAP@0.25 and mAP@0.5 metric, our method achieves the state-of-the-art. In particular, for mAP@0.5, the improvement is even larger than mAP@0.25, that is, we improve by 2.7 points and 3.4 points upon VoteNet and H3DNet respectively. This indicates we can obtain more accurate bounding box prediction with the help of proposed pre-training strategy.

SUN RGB-D. We also conduct the experiments on SUN RGB-D. We report the results in Table 3. With pre-training, we again achieve the state-of-the-art. For mAP@0.25, we improve 1.5 points for both VoteNet and H3DNet. For mAP@0.5, we improve 2.5 points and 4.1 points for VoteNet and H3DNet. This result once again illustrates our method can predict more accurate bounding box. As for the average precision of each class, improvement can be observed for 7 out of 10 categories.

Less Training Data. To show our method can truly learn a better initialization through pre-training, we further conduct the empirical studies with much less training data. We report the results in Table 4. We use 5%, 10%, 25% and 50% of the training data from ScanNetV2 dataset. As can be seen from the Table 4, the improvement under this few-shot setting is still obvious, especially for mAP@0.25. The improvement on mAP@0.25 is even growing larger when less data is used. Notably, the improvement of mAP@0.25 is larger than 5 points when we use less than 10% training data. On the other hand, the improvement on mAP@0.5 is almost unchanged compared to mAP@0.25. This indicates our pre-training method can help the model of downstream high-level tasks to achieve a better coarse understanding of the scene when less data is available. But to gain more accurate understanding, we still need supervised learning with annotated data.

Ablation Study. In Table 5, we conduct three groups ablation studies. All these ablation studies are conducted on ScanNetV2 dataset with VoteNet as the backbone. We use mAP@0.25 as the evaluation metric.

We first study the choice of datasets where the pre-training is performed. From Table 5a, we observe that pre-training on either ShapeNet or ScanNetV2 can both improve the performance. Yet, thanks to the larger scale of ShapeNet, i.e. more samples from more diverse categories, pre-training on it can achieve better results compared to ScanNetV2. Furthermore, we exhibit the possibility to combine both datasets to help the pre-training. Having the objects from both datasets, we can achieve even better fine-tuning result compared to one single dataset is used.

We then study the effect of loss function used for pre-training in Table 5b. Compared to the point-level contrastive loss used by PointContrast, we can achieve even better pre-training results with the instance-level contrastive loss. This indicates the object-level contrastive learning can better help the downstream localization tasks by incorporating more instance-level knowledge. Considering that the label of objects in ShapeNet is easy to access, we also add an additional segmentation loss by assigning all the points of an object with the corresponding object label. This can bring some marginal improvement with additional supervi-

Table 3: 3D object detection results on SUN RGB-D val dataset. We report per-category results of average precision (AP) with 3D IoU threshold 0.25, and mean of AP across all semantic classes with 3D IoU threshold 0.25 and 0.5. For fair comparison, with previous methods, the evaluation is on the SUN RGB-D V1 data.

	Input	bathtub	bed	bkshf	chair	desk	drser	nigtstd	sofa	table	toilet	mAP$_{25}$	mAP$_{50}$
DSS[48]	Geo + RGB	44.2	78.8	11.9	61.2	20.5	6.4	15.4	53.5	50.3	78.9	42.1	-
COG[42]	Geo + RGB	58.3	63.7	31.8	62.2	45.2	15.5	27.4	51.0	51.3	70.1	47.6	-
2D-driven[26]	Geo + RGB	43.5	64.5	31.4	48.3	27.9	25.9	41.9	50.4	37.0	80.4	45.1	-
F-PointNet[36]	Geo + RGB	43.3	81.1	33.3	64.2	24.7	32.0	58.1	61.1	51.1	90.9	54.0	-
PointContrast [57]	Geo	-	-	-	-	-	-	-	-	-	-	57.5	34.8
VoteNet [35]	Geo	74.7	83.0	28.8	75.3	22.0	29.8	62.2	64.0	47.3	90.1	57.7	32.9
Ours + VoteNet	Geo	76.2	83.5	29.2	76.7	25.1	33.2	64.2	63.8	49.0	91.2	59.2	35.4
H3DNet [62]	Geo	73.8	85.6	31.0	76.7	29.6	33.4	65.5	66.5	50.8	88.2	60.1	39.0
Ours + H3DNet	Geo	71.2	86.4	38.7	77.8	28.0	36.5	68.3	67.7	50.3	91.0	**61.6**	**43.1**

Table 4: Effects of the training data size. We show the mean of AP across all semantic classes with 3D IoU threshold 0.25 and 0.5 when training on ScanNetV2 with less data. We report the results of using 5%, 10%, 25% and 50% data.

	100%		50%		25%		10%		5%	
	mAP$_{25}$	mAP$_{50}$	mAP$_{25}$	mAP$_{50}$	mAP$_{25}$	mAP$_{50}$	mAP$_{25}$	mAP$_{50}$	mAP$_{25}$	mAP$_{50}$
VoteNet [35]	58.6	33.5	47.0	25.3	35.5	20.0	25.1	14.3	12.6	3.2
Ours + VoteNet	61.3	36.2	53.0	30.2	38.2	23.2	28.9	17.2	19.1	10.1
H3DNet [62]	67.2	48.1	61.5	40.6	51.6	30.9	37.0	20.7	26.6	11.3
Ours + H3DNet	68.6	51.5	63.2	43.6	54.4	33.5	42.2	23.4	32.0	13.9

sion signal being used. This illustrates the fact that our complete unsupervised pre-training strategy can achieve comparable performance with the supervised pre-training on synthetic dataset.

We finally show the necessity of some strategies used in scene generation. In Table 5c, we verify the necessity of gravity principle and the need of floor and wall in a scene. Without these components, we can still improve upon the baseline, but the larger domain shift between real scene and generated scene may hamper the pre-training from obtaining better model for fine-tuning on the real dataset of downstream tasks.

Comparison with PointContrast. To show our pre-training method is more suitable for the 3D object detection task, we compare with another pre-training method, namely PointContrast, on ScanNetV2 and SUN RGB-D using VoteNet [35] as the detection model, and we use mAP@0.25 as the evaluation metric. The results are reported in Table 6

We find that using Sparse Res-UNet instead of PointNet++ as the backbone model leads to worse detection performance when training from scratch. However, the improvement brought by PointContrast to the detectors based on PointNet++ is quite marginal, and the final performance is on par with the detectors using Sparse Res-UNet as the backbone. On the contrary, considering there is no
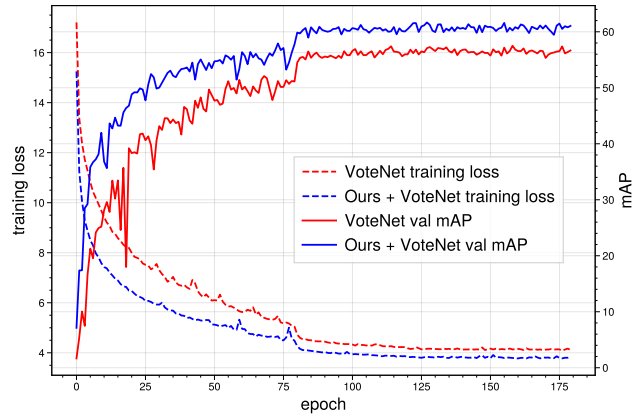

Figure 4: Training from scratch vs. fine-tuning with RandomRooms pre-trained weights. We report the 3D detection training loss and the validation mAP@0.25 of VoteNet on ScanNetV2.

need to keep the point correspondence, our RandomRooms method can learn a much better initialization for the PointNet++ style model, which is stronger backbone for current state-of-the-art 3D object detectors. This demonstrates our method is superior on the object detection task compared to PointContrast.

Learning Curve. We show the learning curve of our method as well as the baseline VoteNet in Figure 4. We ob-

Table 5: Ablation analysis on the proposed RandomRooms method. We investigate the effects of pre-training datasets, learning losses and random room generation methods. We report the mAP$_{25}$ results of VoteNet on ScanNetV2.

(a) Ablation studies on pre-training datasets.

Pre-training dataset	mAP
baseline	58.6
ScanNetV2	60.2
ShapeNet	61.3
ShapeNet + ScanNetV2	61.5

(b) Ablation studies on pre-training losses.

Pre-training loss	mAP
baseline	58.6
point-level contrastive	59.2
instance-level contrastive	61.3
instance-level contrastive + seg.	61.5

(c) Ablation studies on room generation.

Generation method	mAP
baseline	58.6
RandomRooms	61.3
w/o gravity	60.5
w/o floor/wall	60.7

Table 6: We compare our method with PointContrast on ScanNetV2 and SUN R-GBD using PointNet++ as backbone. We show mean of average precision (mAP) across all semantic classes with 3D IoU threshold 0.25.

	ScanNetV2	SUN RGB-D
Sparse Res-UNet w/o pre-training	56.7	55.6
Sparse Res-UNet w/ PointContrast	58.5	57.5
PointNet++ w/o pre-training	58.6	57.7
PointNet++ w/ PointContrast	58.5	57.9
PointNet++ w/ RandomRooms	**61.3**	**59.2**

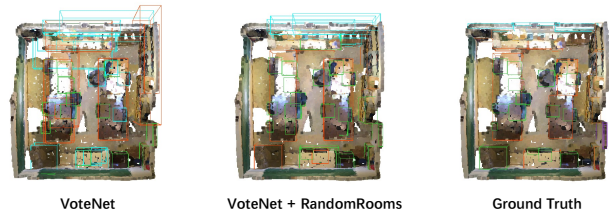VoteNet   VoteNet + RandomRooms   Ground Truth

Figure 5: Visual Results on ScanNetV2. We compare the qualitative detection results with the baseline VoteNet method. The pre-trained model can produce more accurate detection results with less false positives, and is closer to the ground-truth bounding boxes.

serve that our pre-trainig weights significantly help improve the learning speed and stabilize the training process. The model with pre-training weights can achieve lower training loss and better validation mAP, which clearly demonstrates the effectiveness of the proposed method.

Visualization. We visualize the detection results of the baseline VoteNet that is trained from scarch and the pre-trained model using our method on ScanNet. The results are shown in Figure 5. We see the pre-trained model can produce more accurate detection results with less false positives, and is closer to the ground-truth bounding boxes. The visual results further confirm the effectiveness of the proposed method.

Discussions. Though we follow many heuristic rules when generating the *random rooms*, there still exist domain gap between the real scene and generated one. The extensive experimental results shed light on an interesting fact, that is, in 3D representation learning the layout of objects may not be that important for recognition as in 2D vision. We only need to ensure the set of objects can spread out in the space, while the interaction among objects does not matter that much as 2D vision where hidden interactions may play as an important cue for many high-level scene understanding tasks like detection. This may be due to the ovelap is not that severe in complex 3D scenes. We think this may open a path for future research on 3D learning.

5. Conclusion

In this paper, we have proposed a new pipeline, namely RandomRoom, for 3D pre-training that can make use of the synthetic CAD model dataset to help the learning on real dataset on high-level 3D object detection task. Unlike previous works performing contrastive learning at the level of points, we perform contrastive learning at the object level by composing two different scenes with same set of objects that are randomly sampled from the CAD model dataset. Empirically, we show consistent improvements in downstream 3D detection tasks on several base models, especially when less training data are used. Benefiting from the rich semantic knowledge and diverse objects from synthetic data, our method establishes the new state-of-the-art on widely-used 3D detection benchmarks ScanNetV2 and SUN RGB-D. We except this work can open a new path for future research on how to exploit easily accessible synthetic objects for more complex tasks for 3D scene understanding.

A. Details about Random Room Generation

To more clearly show the generation process of random rooms, we provide pseudo-code and explanatory comments of our room generation method in Algorithm 1.

B. Visualization of Random Rooms

We show more examples of the generated random room pairs in Figure 6.

References

[1] Angel X Chang, Thomas Funkhouser, Leonidas Guibas, Pat Hanrahan, Qixing Huang, Zimo Li, Silvio Savarese, Manolis Savva, Shuran Song, Hao Su, et al. Shapenet: An information-rich 3d model repository. *arXiv preprint arXiv:1512.03012*, 2015. 2, 5

[2] Ting Chen, Simon Kornblith, Mohammad Norouzi, and Geoffrey Hinton. A simple framework for contrastive learning of visual representations. *ICML*, 2020. 3, 5

[3] Xinlei Chen, Haoqi Fan, Ross Girshick, and Kaiming He. Improved baselines with momentum contrastive learning. *arXiv preprint arXiv:2003.04297*, 2020. 3, 5

[4] Christopher Choy, JunYoung Gwak, and Silvio Savarese. 4d spatio-temporal convnets: Minkowski convolutional neural networks. In *CVPR*, pages 3075–3084, 2019. 1

[5] Angela Dai, Angel X Chang, Manolis Savva, Maciej Halber, Thomas Funkhouser, and Matthias Nießner. Scannet: Richly-annotated 3d reconstructions of indoor scenes. In *CVPR*, pages 5828–5839, 2017. 4, 5

[6] Haowen Deng, Tolga Birdal, and Slobodan Ilic. Ppf-foldnet: Unsupervised learning of rotation invariant 3d local descriptors. In *ECCV*, pages 602–618, 2018. 2, 3

[7] Jia Deng, Wei Dong, Richard Socher, Li-Jia Li, Kai Li, and Li Fei-Fei. Imagenet: A large-scale hierarchical image database. In *CVPR*, pages 248–255, 2009. 3

[8] Jacob Devlin, Ming-Wei Chang, Kenton Lee, and Kristina Toutanova. Bert: Pre-training of deep bidirectional transformers for language understanding. In *NAACL*, 2019. 3

[9] Alexey Dosovitskiy, Philipp Fischer, Jost Tobias Springenberg, Martin Riedmiller, and Thomas Brox. Discriminative unsupervised feature learning with exemplar convolutional neural networks. *T-PAMI*, 38(9):1734–1747, 2015. 3

[10] Gil Elbaz, Tamar Avraham, and Anath Fischer. 3d point cloud registration for localization using a deep neural network auto-encoder. In *CVPR*, 2017. 2, 3

[11] Matheus Gadelha, Rui Wang, and Subhransu Maji. Multiresolution tree networks for 3d point cloud processing. In *ECCV*, pages 103–118, 2018. 2, 3

[12] Ross Girshick. Fast r-cnn. In *ICCV*, pages 1440–1448, 2015. 3

[13] Ross Girshick, Jeff Donahue, Trevor Darrell, and Jitendra Malik. Rich feature hierarchies for accurate object detection and semantic segmentation. In *CVPR*, pages 580–587, 2014. 3

[14] Jean-Bastien Grill, Florian Strub, Florent Altché, Corentin Tallec, Pierre Richemond, Elena Buchatskaya, Carl Doersch,

Bernardo Avila Pires, Zhaohan Guo, Mohammad Gheshlaghi Azar, et al. Bootstrap your own latent-a new approach to self-supervised learning. *NeurIPS*, 33, 2020. 3

[15] Raia Hadsell, Sumit Chopra, and Yann LeCun. Dimensionality reduction by learning an invariant mapping. In *CVPR*, volume 2, pages 1735–1742. IEEE, 2006. 3

[16] Kaveh Hassani and Mike Haley. Unsupervised multi-task feature learning on point clouds. In *ICCV*, 2019. 3

[17] Kaiming He, Haoqi Fan, Yuxin Wu, Saining Xie, and Ross Girshick. Momentum contrast for unsupervised visual representation learning. In *CVPR*, pages 9729–9738, 2020. 3, 5

[18] Olivier J Hénaff, Ali Razavi, Carl Doersch, SM Eslami, and Aaron van den Oord. Data-efficient image recognition with contrastive predictive coding. *arXiv preprint arXiv:1905.09272*, 2019. 3

[19] Ji Hou, Angela Dai, and Matthias Nießner. 3d-sis: 3d semantic instance segmentation of rgb-d scans. In *CVPR*, 2019. 1, 2, 5, 6

[20] Jeremy Howard and Sebastian Ruder. Universal language model fine-tuning for text classification. In *ACL*, 2018. 3

[21] Zeyu Hu, Mingmin Zhen, Xuyang Bai, Hongbo Fu, and Chiew-lan Tai. JSENet: Joint semantic segmentation and edge detection network for 3D point clouds. In *ECCV*, 2020. 1

[22] Li Jiang, Hengshuang Zhao, Shaoshuai Shi, Shu Liu, Chi-Wing Fu, and Jiaya Jia. PointGroup: Dual-Set Point Grouping for 3D Instance Segmentation. In *CVPR*, pages 4867–4876, 2020. 2

[23] Diederik P Kingma and Jimmy Ba. Adam: A method for stochastic optimization. *arXiv preprint arXiv:1412.6980*, 2014. 5

[24] Roman Klokov and Victor Lempitsky. Escape from cells: Deep kd-networks for the recognition of 3d point cloud models. In *ICCV*, pages 863–872, 2017. 1, 2

[25] Abhijit Kundu, Xiaoqi Yin, Alireza Fathi, David Ross, Brian Brewington, Thomas Funkhouser, and Caroline Pantofaru. Virtual multi-view fusion for 3d semantic segmentation. In *ECCV*, 2020. 1

[26] Jean Lahoud and Bernard Ghanem. 2d-driven 3d object detection in rgb-d images. In *ICCV*, 2017. 5, 7

[27] Jiaxin Li, Ben M Chen, and Gim Hee Lee. So-net: Self-organizing network for point cloud analysis. In *CVPR*, pages 9397–9406, 2018. 1, 2

[28] Peiliang Li, Xiaozhi Chen, and Shaojie Shen. Stereo r-cnn based 3d object detection for autonomous driving. In *CVPR*, pages 7644–7652, 2019. 1, 2

[29] Yangyan Li, Rui Bu, Mingchao Sun, Wei Wu, Xinhan Di, and Baoquan Chen. Pointcnn: Convolution on x-transformed points. In *NeurIPS*, pages 828–838, 2018. 1, 2

[30] Tsung-Yi Lin, Michael Maire, Serge Belongie, James Hays, Pietro Perona, Deva Ramanan, Piotr Dollár, and C Lawrence Zitnick. Microsoft coco: Common objects in context. In *ECCV*, pages 740–755. Springer, 2014. 1

[31] Xinhai Liu, Zhizhong Han, Xin Wen, Yu-Shen Liu, and Matthias Zwicker. L2g auto-encoder: Understanding point clouds by local-to-global reconstruction with hierarchical

self-attention. In *ACM MM*, pages 989–997. ACM, 2019. 2

[32] Yongcheng Liu, Bin Fan, Shiming Xiang, and Chunhong Pan. Relation-shape convolutional neural network for point cloud analysis. In *CVPR*, pages 8895–8904, 2019. 4

[33] Matthew E Peters, Mark Neumann, Mohit Iyyer, Matt Gardner, Christopher Clark, Kenton Lee, and Luke Zettlemoyer. Deep contextualized word representations. In *NAACL*, 2018. 3

[34] Gilles Puy, Alexandre Boulch, and Renaud Marlet. FLOT: Scene Flow on Point Clouds guided by Optimal Transport. In *ECCV*, 2020. 2

[35] Charles R Qi, Or Litany, Kaiming He, and Leonidas J Guibas. Deep hough voting for 3d object detection in point clouds. In *Proceedings of the IEEE International Conference on Computer Vision*, pages 9277–9286, 2019. 2, 5, 6, 7

[36] Charles R Qi, Wei Liu, Chenxia Wu, Hao Su, and Leonidas J Guibas. Frustum pointnets for 3d object detection from rgb-d data. In *CVPR*, pages 918–927, 2018. 2, 5, 6, 7

[37] Charles R Qi, Hao Su, Kaichun Mo, and Leonidas J Guibas. Pointnet: Deep learning on point sets for 3d classification and segmentation. *CVPR*, 1(2):4, 2017. 2, 4

[38] Charles Ruizhongtai Qi, Li Yi, Hao Su, and Leonidas J Guibas. Pointnet++: Deep hierarchical feature learning on point sets in a metric space. In *NeurIPS*, pages 5099–5108, 2017. 2, 4

[39] Alec Radford, Karthik Narasimhan, Tim Salimans, and Ilya Sutskever. Improving language understanding by generative pre-training, 2018. 3

[40] Yongming Rao, Jiwen Lu, and Jie Zhou. Global-local bidirectional reasoning for unsupervised representation learning of 3d point clouds. In *CVPR*, pages 5376–5385, 2020. 2, 3

[41] Shaoqing Ren, Kaiming He, Ross Girshick, and Jian Sun. Faster r-cnn: Towards real-time object detection with region proposal networks. In *NeurIPS*, pages 91–99, 2015. 3

[42] Zhile Ren and Erik B Sudderth. Three-dimensional object detection and layout prediction using clouds of oriented gradients. In *CVPR*, pages 1525–1533, 2016. 5, 7

[43] Florian Schroff, Dmitry Kalenichenko, and James Philbin. Facenet: A unified embedding for face recognition and clustering. In *CVPR*, pages 815–823, 2015. 3

[44] Shaoshuai Shi, Chaoxu Guo, Li Jiang, Zhe Wang, Jianping Shi, Xiaogang Wang, and Hongsheng Li. PV-RCNN: Point-Voxel Feature Set Abstraction for 3D Object Detection. In *CVPR*, 2020. 1, 2

[45] Shaoshuai Shi, Xiaogang Wang, and Hongsheng Li. Pointrcnn: 3d object proposal generation and detection from point cloud. In *CVPR*, pages 770–779, 2019. 1, 2

[46] Kihyuk Sohn. Improved deep metric learning with multiclass n-pair loss objective. In *NeurIPS*, pages 1857–1865, 2016. 3

[47] Shuran Song, Samuel P Lichtenberg, and Jianxiong Xiao. Sun rgb-d: A rgb-d scene understanding benchmark suite. In *CVPR*, pages 567–576, 2015. 2, 5

[48] Shuran Song and Jianxiong Xiao. Deep sliding shapes for amodal 3d object detection in rgb-d images. In *CVPR*, 2016. 5, 6, 7

[49] Hugues Thomas, Charles R Qi, Jean-Emmanuel Deschaud, Beatriz Marcotegui, Francois Goulette, and Leonidas J Guibas. Kpconv: Flexible and deformable convolution for point clouds. *ICCV*, 2019. 2

[50] Yonglong Tian, Dilip Krishnan, and Phillip Isola. Contrastive multiview coding. *arXiv preprint arXiv:1906.05849*, 2019. 3

[51] Yonglong Tian, Chen Sun, Ben Poole, Dilip Krishnan, Cordelia Schmid, and Phillip Isola. What makes for good views for contrastive learning. *arXiv preprint arXiv:2005.10243*, 2020. 3

[52] Weiyue Wang, Ronald Yu, Qiangui Huang, and Ulrich Neumann. Sgpn: Similarity group proposal network for 3d point cloud instance segmentation. In *CVPR*, pages 2569–2578, 2018. 2

[53] Yue Wang, Yongbin Sun, Ziwei Liu, Sanjay E. Sarma, Michael M. Bronstein, and Justin M. Solomon. Dynamic graph cnn for learning on point clouds. *TOG*, 2019. 1, 2

[54] Yi Wei, Shaohui Liu, Wang Zhao, and Jiwen Lu. Conditional single-view shape generation for multi-view stereo reconstruction. In *CVPR*, pages 9651–9660, 2019. 2

[55] Zhirong Wu, Shuran Song, Aditya Khosla, Fisher Yu, Linguang Zhang, Xiaoou Tang, and Jianxiong Xiao. 3d shapenets: A deep representation for volumetric shapes. In *CVPR*, pages 1912–1920, 2015. 4

[56] Zhirong Wu, Yuanjun Xiong, Stella X Yu, and Dahua Lin. Unsupervised feature learning via non-parametric instance discrimination. In *CVPR*, pages 3733–3742, 2018. 3

[57] Saining Xie, Jiatao Gu, Demi Guo, Charles R Qi, Leonidas J Guibas, and Or Litany. Pointcontrast: Unsupervised pre-training for 3d point cloud understanding. *ECCV*, 2020. 2, 3, 4, 5, 6, 7

[58] Yaoqing Yang, Chen Feng, Yiru Shen, and Dong Tian. Foldingnet: Point cloud auto-encoder via deep grid deformation. In *CVPR*, pages 206–215, 2018. 2, 3

[59] Zetong Yang, Yanan Sun, Shu Liu, and Jiaya Jia. 3dssd: Point-based 3d single stage object detector. In *CVPR*, pages 11040–11048, 2020. 1, 2

[60] Li Yi, Wang Zhao, He Wang, Minhyuk Sung, and Leonidas J Guibas. Gspn: Generative shape proposal network for 3d instance segmentation in point cloud. In *CVPR*, 2019. 5, 6

[61] Andy Zeng, Shuran Song, Matthias Nießner, Matthew Fisher, Jianxiong Xiao, and Thomas Funkhouser. 3dmatch: Learning local geometric descriptors from rgb-d reconstructions. In *CVPR*, 2017. 2, 3

[62] Feihu Zhang, Jin Fang, Benjamin Wah, and Philip Torr. Deep fusionnet for point cloud semantic segmentation. In *ECCV*, 2020. 1, 7

[63] Zaiwei Zhang, Bo Sun, Haitao Yang, and Qixing Huang. H3dnet: 3d object detection using hybrid geometric primitives. In *ECCV*, 2020. 2, 5, 6

Algorithm 1 Pseudo-code of Random Room Generation

```
1  # objects: list of object point clouds
2
3  # object level data augmentation
4  objcts = object_augmentation(objcts)
5
6  # sort objects by their areas
7  objects, object_ind, obj_area = sort_object(objects)
8
9  # set the overall area of the rectangular room
10 overall_area = sum(obj_area) * 2 * 10000 * (random.random() * 0.4 + 0.6)
11 a_value = np.sqrt(overall_area)
12 a = random.randint(int(a_value*0.75), int(a_value*1.25))
13 b = int(overall_area) // a
14 a_m = float(a) / 100.
15 b_m = float(b) / 100.
16 room_state = np.zeros((a, b), dtype=np.float)
17
18 final_layout = []
19 instance_label = []
20
21 # place object to the room
22 for i in range(len(objcts)):
23     obj = objects[i]
24     x, y, z = get_object_size(obj)
25
26     for _ in range(max_iter):
27         # generate the position from beta distribution
28         pos_x = np.random.beta(0.5, 0.5) * (a_m - x)
29         pos_y = np.random.beta(0.5, 0.5) * (b_m - y)
30         state_part = room_state[int(pos_x*100):int((pos_x+x)*100), int(pos_y*100): int((pos_y+y)*100)]
31         max_height = state_part.max()
32         if (max_height + z < 2.0 and max_height < 0.5) or max_height < 1e-3:
33             break
34
35     room_state[int(pos_x * 100):int((pos_x + x) * 100), int(pos_y * 100): int((pos_y + y) * 100)] += z
36     obj[:, 0] += pos_x
37     obj[:, 1] += pos_y
38     obj[:, 2] += max_height
39     final_layout.append(obj)
40     instance_label.append(np.ones((obj.shape[0],), dtype=int) * (object_ind[i] + 1))
41
42 # add floor and walls
43 final_layout, instance_label = add_floor_wall(final_layout, instance_label)
44
45 # form the final scene point cloud
46 final_layout = np.concatenate(final_layout, axis=0)
47 instance_label = np.concatenate(instance_label, axis=0)
48
49 # normalize coordinates
50 final_layout[:, 0:2] = final_layout[:, 0:2] - final_layout[:, 0:2].mean(axis=0, keepdims=True)
```

Figure 6: Visualization of the pairs of *Random Rooms*.